

Vibration Analysis of Rolling Element Bearings Defects

H. Saruhan^{*1}, S. Saridemir², A. Çiçek³ and İ. Uygur⁴

^{1,4} Düzce University
Faculty of Engineering
Düzce, Turkey

*hamitsaruhan@duzce.edu.tr

^{2,3} Düzce University
Faculty of Technology
Düzce, Turkey

ABSTRACT

In this work, vibration analysis of rolling element bearings (REBs) defects is studied. The REBs are the most widely used mechanical parts in rotating machinery under high load and high rotational speeds. When the defect in a rolling element comes into contact with another element surface, an impact force is generated which is resulting in an impulsive response of the bearing. A defect at any element of the REB transmits to all other elements such as outer race, inner race, ball and, train cage of the bearing. The defect in rolling elements may lead to serious catastrophic consequences resulting in costly downtime. For this purpose, the vibration analysis technique which is a reliable and accurately detecting defect in the bearing elements is used. The vibration data captured and used for determination and validation is composed from four different defects states of the REB -outer raceway defect, inner raceway defect, ball defect, and combination of the bearing elements defect- and one representing normal state of the bearing for four different running speeds with two load levels. The results obtained from the experiments have illustrated and explained.

Keywords: Rolling element bearing, bearing elements defect, vibration spectrum analysis

1. Introduction

A large majority of rotating machineries rely on rolling element bearings (REBs). Due to necessity and vital contribution to most rotating machineries, the requirements on the bearings have become stricter everyday. The bearings provide relative positioning and rotating freedom while usually transmitting a load between shaft and housing [1]. Rotating machineries are complex and have numerous components that could potentially fail. An analysis should be made to identify the bearings defects before they become catastrophically fail with the associated downtime costs and significant damage to other parts of rotating machineries. The vibration spectrum analysis is a popular technique among others such as time domain and time frequency domain for tracking machinery operating conditions. Intensive research [2-6] has been done in recent years for the REBs defect diagnosis to ensure the performance and extend the bearing life. In this study, the different type of the REB defects cases with respected to two different load level is taken in account since the load affects the defect

signature magnitude. The results obtained from the experiments have illustrated and explained.

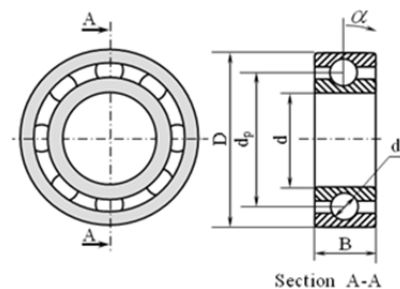


Figure 1. Geometry and dimensions of a ball bearing.

2. Bearing Defects

The geometry and dimensions of the REB which consists of outer race, inner race, and balls are shown in Fig. 1. Defects in the REB produce a series of impacts which repeat periodically at a rate known as the bearing frequencies.

The different defects occurring in the REB can be classified according to the damaged elements as: outer raceway defect, inner raceway defect, ball defect, and combination of bearing components defect. Each bearing element has a characteristic defect frequency that depends on mechanical dimensions of the bearing. The product of multipliers with the shaft rotational speed gives the defect frequency of bearing running at given shaft speed [7].

By identifying the type of the bearing characteristics frequency, the cause of the defect can be determined [8]. The bearing frequency multipliers equations provide a theoretical estimate of the frequency to be expected when the bearing elements defect takes place. To calculate these frequency multipliers for the REB in which the inner race rotates and the outer race is stationary, the following Eq. (1-3) are used [7].

$$BPFO = (N_b / 2) \left(1 - (N_b / d_p) \cos \alpha \right) \quad (1)$$

$$BPFI = (N_b / 2) \left(1 + (N_b / d_p) \cos \alpha \right) \quad (2)$$

$$BSF = (d_p / 2d_b) \left(1 - \left((d_b / d_p) \cos \alpha \right)^2 \right) \quad (3)$$

where *BPFO* is ball pass frequency multiplier of the outer race, *BPFI* is ball pass frequency multiplier of the inner race, *BSF* is ball spin frequency multiplier, N_b is number of rolling elements, d_b is rolling element diameter, d_p is pitch diameter, and α is contact angle which is the angle of load from the radial plane.

3. Experimental Setup

The test rig for the experiments is shown in Fig. 2. The rig consists of a shaft with length of 850 mm and diameter of 19.05 mm. The shaft is coupled with a flexible coupling to minimize the effect of the high frequency vibration generated by the ½ HP motor. A three-phase AC induction motor is connected to a variable speed control unit for achieving variable speeds.

The motor can be run in the speed range of 0-3600 rpm. Two bearings are fitted in to the mounting housings. The normal state and defected bearings are installed in the inboard bearing housing for collecting data. Also the normal state bearing is installed in the outboard bearing housing for all the test cases. MB ER-12K type of ball bearings is utilized in the test rig. A static load is applied by two aluminum disks with 151.8 mm diameter and 0.668 kg weight for each. A loader weighting 5.04 kg is used in order to load the bearings for enhancing the spectrum amplitude of the system. The vibration of the bearing in the vertical and horizontal directions (x and y) is measured by four (608A11) accelerometers with a sensitivity of 100 mV/g and frequency range of 0.5 to 10 kHz.

The accelerometers are mounted at 90° on the bearing housings. The system is composed of DAQ (Data Acquisition) card provides four channels for vibratory response acquisition and one channel for rotational speed acquisition. DAQ channels were set as CH1 and CH2 for normal state bearing fitted in outboard bearing housing in vertical and horizontal directions respectively while CH3 and CH4 for normal state and defected bearings fitted in inboard bearing housing in vertical and horizontal directions respectively.

All channels are simultaneous. PCI bus ensures high speed (102.4 K samples/sec.) DAQ. The data were collected using the VibraQuest™ software and hardware system. The data collection system consists of a high bandwidth amplifier designed for the vibration signals. The data recorder is equipped with low-pass filters at the input stage for anti-aliasing.

The parameters detail of the bearing used are given in Table 1. It should be noted that five conditions of bearing - normal state bearing, bearing with ball defect, bearing with inner race defect, bearing with outer race defect, and combination of bearing elements defect- have been considered. As a first step, the experiment was utilized for normal state bearing in order to establish the base-line data. Then data is collected for others four different defect conditions of the REB.

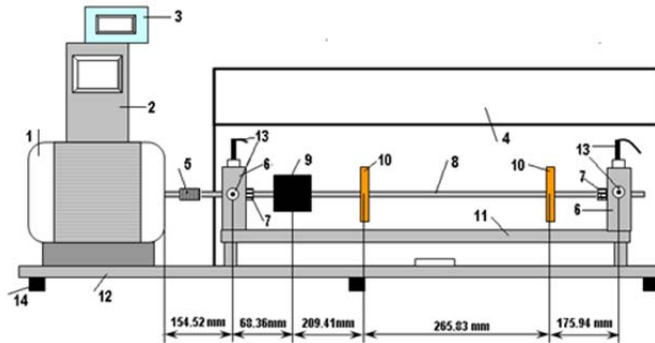


Figure 2. Experimental test rig: (1) ½ HP Motor; (2) Variable speed controller; (3) Tachometer; (4) Safety cover (5)Flexible coupling; (6) Bearing housing; (7) Bearing; (8) Shaft; (9) Loader; (10) Disk; (11) Extended rotor deck; (12) Base; (13) Accelerometer; (14) Rubber isolators.

Bearing Specification	MB ER-12K
Outer diameter, D (mm)	47.00016
Inner diameter, d (mm)	19.05
Pitch diameter, d_p (mm)	33.50006
Ball diameter, d_b (mm)	7.9375
Outer ring width, B (mm)	15.8496
Number of ball, N_b	8
Contact angle, α (degree)	0°

Table 1. The ball bearing parameters detail.

4. Results and Discussions

Fitting the parameter of deliberately defected bearing MB ER-12K into Eq. (1-3), the BPFO is calculated as 3.0522. Similarly, it is 4.9477 for the BPFI and 1.9917 for the BSF. Although the REBs are manufactured using high technology, like any other manufactured machine parts they will have degrees of imperfection and generate vibration.

Vibration frequency multipliers given by manufacturer for the normal state bearing MB ER-12K are 0.0508 for the BPFO, 0.0825 for the BPFI, and 0.0332 for the BSF. Table 2 shows defect frequencies of the REB for the shaft running speed 17 Hz (1020 rpm). It can be seen that agreement between the theoretical and measured fault data is found to be remarkably good.

MB ER-12K	Defect frequency, Hz		
	Normal State Bearing	Defected Bearing	
		Theoretical	Measured
BPFO	0.8636	51.88	50.00
BPFI	1.4025	84.11	82.81
BSF	0.5644	33.85	32.81

Table 2. Defect frequencies of the REB for running speed 17 Hz.

The REB represents a complex vibration system. The vibrations are recorded from the bearing housing in vertical and horizontal directions. The vibration signal measured vertically is utilized for analysis whereas the signal measured from the horizontal direction is used for the verification. The vibration signals are collected at frequency limit of 5 kHz. Frequency limit indicates that how fast the data will be taken. Each test trial consists of 19.84 second duration. The resolution was 3200 spectra lines using Hanning window.

The resolution of a spectrum indicates the number of lines used to plot the spectrum. The sampling rate equals frequency limit, which determines how fast the data will be taken, multiply 2.56 for the software used. Thus, the sampling rate was set as 12800 (= 5 kHz x 2.56). The first series data was collected from each of test bearings mounted in the inboard housing. Test bearings are normal state bearing with outer raceway defect, bearing with inner raceway defect, bearing with ball defect, and combination of bearing elements defect when no load attached to the disks.

Each bearing is tested under four different shaft running speeds (17 Hz, 25 Hz, 33 Hz, and 41 Hz). The second series of data was collected when the load (5.04 kg) was attached to the disks for the same running speeds and bearing elements defect conditions.

The repetitive of the vibration signals is displayed in the frequency spectrum.

Generally the low frequency band (<1 kHz) includes the bearing pass frequencies and the high frequency band (1 ~10 kHz) indicates the natural frequencies [9]. Monitoring the frequencies harmonics at frequency range (<5 kHz) has been successful in bearing diagnosis [10,11]. Table 3 gives the measuring of the maximum amplitude value of the vibration spectrum captured in linear scale between 0 and 5 kHz. Table 3 indicates that loader weight with different shaft running speed affect the peak amplitude value.

Formulae should be integrated within the text, centered. They should be in 10-point Arial or Symbol regular font. Please use earlier versions of Word up to 2003 (or 2004 for the Macintosh) or the legacy equation editor in Word 2007, 2008 for Mac. Long equations should be set off from the text and numbered sequentially. After an equation is introduced, refer to it by number (e.g., "Eq. 1," "Eqs. 3 and 4").

The bearing defects results in harmonic, multiples of frequency, of the defected frequencies in the vibration spectrum. The repetitive of the vibration signal of defects can be observed as peaks in the frequency spectrum. The root mean square (RMS) value have been applied in diagnosing the bearings

Type of Bearing	Maximum amplitude spectrum value of vibration response peaks (gPk)							
	17Hz		25Hz		33Hz		41Hz	
	Freq.	Amp.	Freq.	Amp.	Freq.	Amp.	Freq.	Amp.
Two disks and without loader								
GOOD	57.81	0.000564	75.00	0.003604	32.81	0.002636	365.62	0.004281
OUTER	50.00	0.001029	25.00	0.002313	164.06	0.002546	81.25	0.003289
INNER	645.31	0.004197	342.19	0.006606	323.87	0.012786	643.75	0.010620
BALL	50.00	0.000912	75.00	0.008599	32.81	0.004288	40.62	0.006150
COMB	498.44	0.000477	25.00	0.003273	32.81	0.003260	40.62	0.004841
Two disk with loader								
GOOD	50.00	0.001092	25.00	0.004217	32.81	0.004999	40.62	0.008106
OUTER	50.00	0.005932	50.00	0.007086	48.44	0.004649	40.62	0.005058
INNER	50.00	0.005069	50.00	0.003290	321.87	0.010890	400.0	0.013565
BALL	50.00	0.003886	73.44	0.005200	32.81	0.004329	162.5	0.009527
COMB	50.00	0.001378	25.00	0.002146	50.00	0.007570	40.62	0.005898

Table 3. Maximum amplitude spectrum value of vibration response peaks.

Running Speed		Corresponding Frequency (xHz)														
17 Hz		x1	x2	x3	x4	x5	x6	x7	x8	x9	x10	x11	x12	x13		
Calculated	With Defect	BPFO	51.8	103.7	155.6	207.5	259.4	311.3	363.2	415.0	466.9	518.8	570.7	622.6	674.5	
		BPFI	84.1	168.2	252.3	336.4	420.5	504.6	588.7	672.8	756.9	841.1	925.2	1009.3	1093.4	
		BSF	33.8	67.7	101.5	135.4	169.2	203.1	237.0	270.8	304.7	338.5	372.4	406.3	440.1	
	GOOD	BPFO	0.86	1.72	2.59	3.45	4.31	5.18	6.04	6.90	7.77	8.63	9.49	10.36	11.22	
		BPFI	1.40	2.80	4.20	5.61	7.01	8.41	9.81	11.22	12.62	14.02	15.42	16.83	18.23	
		BSF	0.56	1.12	1.69	2.25	2.82	3.38	3.95	4.51	5.07	5.64	6.20	6.77	7.33	
	Experiment (two disks without loader)	OUTER	BPFO	50			200	250				450	500	550		
			BPFI	82.81	165.62		331.25		496.87			745.31		910.93		1076.56
			BSF	32.81	65.62							295.31	328.12	360.93		426.56
INNER		BPFO	50	100	150											
		BPFI		162.62	248.43	331.25	414.06	496.87		662.5		828.12	910.93	993.75	1076.56	
		BSF	32.81													
BALL		BPFO	50			200										
		BPFI	82.81						579.68					993.75	1076.56	
		BSF	32.81							262.5						
COMB		BPFO	50		150				350		450				650	
		BPFI	82.81	165.62			414.06	496.87						993.75	1076.56	
		BSF	32.81			131.25	164.06	196.87	229.68			328.12		393.75		
Experiment (two disks with loader)		OUTER	BPFO	50	100	150	200	250	300	350	400	450	500	550	600	650
			BPFI	82.87		248.43				496.87	579.68	662.5		828.12	910.93	993.75
			BSF	32.81			131.25		196.87	229.68	262.50		328.12	360.93	393.75	426.56
		INNER	BPFO	50	100	150			300	350	400	450	500	550		
			BPFI	82.81			331.25	414.06	496.87		662.50	745.31	828.12	910.93	993.75	
			BSF	32.81	65.62			164.06		229.68		295.31	328.12	360.93	393.75	426.56
	BALL	BPFO	50	100	150	200	250	300	350	400	450			600		
		BPFI	82.81	165.62	248.43			496.87		662.5	745.31	828.12	910.93		1076.56	
		BSF	32.81						229.68		295.31			393.75	426.56	
	COMB	BPFO	50	100	150	200	250	300	350	400	450				650	
		BPFI	82.81				414.06	496.87		662.50		828.12		993.75	1076.56	
		BSF	32.81	65.62				196.87		262.5			360.93	393.75		

Table 4. The harmonics of defected bearing elements frequencies for running speed 17 Hz.

as an indicator of average of the overall amplitude level of vibration signals at the bearing housing. The vibration spectrum data used for the analysis is for four different defects state of the REB and one representing the normal state of the bearing.

For this study, 40 different test cases (5 bearings of different health conditions and 4 different running speeds with 2 load levels) are examined. In each bearing case, the spectrum values and harmonics of the BPFO, the BPFI, and the BSF are collected and presented in Table 4, 5, 6, and 7. The bearings defect harmonics at frequencies range of 1 to 13X shaft running speed rate are presented in the Tables. As seen in Tables, the

most identified characteristics frequencies are for the inner race defect in combination of bearing elements defect (COMB) case for all running speeds. Thus, the harmonic frequencies for the inner race are found to be quite distinct in comparison to other defected bearing elements.

Also, it should be noted that the amplitude values of the spectrum of the inner raceway defect is much less than the others defects in the COMB case. This is because of difficult transmission path due to more structural interfaces such as ball, oil film, outer race, and bearing housing before reaching the accelerometer.

It can be noted that the spectrum do not contains all harmonics of the shaft running speeds with frequency multipliers and probably influenced by modulations of other vibrations.

There are a number of factors that contribute to the complexity of the bearing signature so that some of the harmonics can not be distinguished clearly. Running speed and load levels (the location of the disks and loader) greatly affected frequencies to deviate from the harmonics range so it is difficult to identify the type of defect in all harmonic peaks.

Also some of harmonics components coincide in frequency with the bearing vibration cause a difficulty to identify the type of defect. In the case of the COMB defects, the spectrum contained the harmonics of the bearing frequency and changed depending on the relative positions of the defects.

It can be seen in Table 4, 5, 6, and 7 that defects are detected when with and without the loader attached to the disks.

For the bearing outer raceway defect (OUTER) case, the vibration transmission path to the transducer is the shortest compared with the bearing inner raceway defect (INNER) and the bearing ball defect (BALL) cases. In Tables, it can be noted that the spectrum data obtained for the BALL especially the case without loader does not reveal harmonics of the defected frequencies distinctively.

Thus, the BALL contains fewer harmonics of the frequencies. The defect may not be in contact with the races all time due to a free spin in any direction. Also the BPFO harmonics are clearly identified confirming the presence of defect in the outer race.

Running Speed		Corresponding Frequency (xHz)														
25 Hz		x1	x2	x3	x4	x5	x6	x7	x8	x9	x10	x11	x12	x13		
Calculated	With Defect	BPFO	76.3	152.6	228.9	305.2	381.5	457.8	534.1	610.4	686.7	763.0	839.3	915.6	991.9	
		BPFI	123.6	247.3	371.0	494.7	618.4	742.1	865.8	989.5	1113.2	1236.9	1360.6	1484.3	1608.0	
		BSF	49.7	99.5	149.3	199.1	248.9	298.7	348.5	398.34	448.13	497.92	547.71	597.51	697.09 5	
	GOOD	BPFO	1.27	2.54	3.81	5.08	6.35	7.62	8.89	10.16	11.43	12.7	13.97	15.24	16.51	
		BPFI	2.06	4.12	6.18	8.25	10.31	12.37	14.43	16.50	18.56	20.62	22.68	24.75	26.81	
		BSF	0.83	1.66	2.49	3.32	4.15	4.98	5.81	6.64	7.47	8.30	9.13	9.96	10.79	
Experiment (two disks without loader)	OUTER	BPFO	75	150			375	450	525	600		750		900	975	
		BPFI	123.43	246.87	370.31							1110.9	1234.3		1481.2	1604.6
		BSF	50		150						400	450	500		600	
	INNER	BPFO	75	150								750				
		BPFI	123.43	246.87			617.18	740.62	864.06	987.5					1481.2	
		BSF	50	100	150							500	550			650
	BALL	BPFO	75					450		600	675				900	975
		BPFI	123.43	246.87		493.75	617.18							1357.8	1481.2	
		BSF	50	100						400	450					650
	COMB	BPFO	75	150		300		450	525		675	750	825	900		
		BPFI	123.43	246.87	370.31		617.18	740.62	864.06	987.5	1110.9	1234.3	1357.8			1604.6
		BSF			150			300			450	500				
Experiment (two disks with loader)	OUTER	BPFO	75	150			375		525	600	675	750	825		975	
		BPFI	123.43	246.87	370.31	493.75			740.62	864.06	987.5	1110.9	1234.3	1357.8		1604.6
		BSF	50		150		250				400		550	600	650	
	INNER	BPFO	75					450	525	600				825	975	
		BPFI	123.43	246.87	370.31	493.75			864.06	987.5	1110.9			1357.8		
		BSF	50				250			400	450					650
	BALL	BPFO				300	375		525				825	900		
		BPFI	123.43	246.87						987.5		1234.3				1604.6
		BSF	50			200	250	300				500	550			
	COMB	BPFO	75		225	300	375	450			675					975
		BPFI	123.43	246.87	370.31	493.75			864.06	987.5	1110.9	1234.3	1357.8	1481.2	1604.6	
		BSF	50	100		200	250	300		400	450	500				650

Table 5. The harmonics of defected bearing elements frequencies for running speed 25 Hz.

		Running Speed		Corresponding Frequency (xHz)												
		33 Hz		x1	x2	x3	x4	x5	x6	x7	x8	x9	x10	x11	x12	x13
Calculated	With Defect	BPFO	100.7	201.4	302.1	402.8	503.6	604.3	705.0	805.7	906.5	1007.9	1107.9	1208.6	1309.3	
		BPFI	163.2	326.5	489.8	653.0	816.3	979.6	1142.9	1632.7	1796.0	1959.2	2122.5	2285.8	2449.1	
		BSF	65.72	131.45	197.17	262.9	328.6	394.3	460.0	525.8	591.5	657.2	722.9	788.7	854.4	
	GOOD	BPFO	1.67	3.35	5.02	6.70	8.38	10.65	11.73	13.41	15.08	16.76	18.44	20.11	21.79	
		BPFI	2.72	5.44	8.16	10.89	13.61	16.33	19.05	21.78	24.50	27.22	29.94	32.67	35.39	
		BSF	1.09	2.19	3.28	4.38	5.47	6.57	7.66	8.76	9.86	10.95	12.05	13.14	14.24	
	Experiment (two disks without loader)	OUTER	BPFO	98.43	196.87			492.18	590.62	689.06		885.93	984.37		1181.2	1279.6
			BPFI	164.06	328.12	492.18	656.25		984.37	1148.4		1476.5	1640.6		1968.7	
			BSF	165.62	131.25	196.87	262.50	328.12			525	590.6	656.25			
INNER		BPFO	98.43		295.31	393.75	492.18			787.5	885.93	984.37	1082.8			
		BPFI	164.06	328.12	492.18			984.37				1640.6				
		BSF	65.62	131.25	196.87	262.50	328.12	393.75		525.0			721.87	787.5		
BALL		BPFO	98.43	196.87					689.06	787.5	885.93	984.37	1082.8			
		BPFI							1148.4	1312.5	1476.5		1804.6			
		BSF	65.62	131.24	196.87	262.50			459.37					787.5		
COMB		BPFO	98.43	196.87			492.18	590.62	689.06		885.93	984.37			1279.6	
		BPFI		328.12	492.18	656.25	820.31	984.37		1312.5	1476.5		1804.6		2132.8	
		BSF	65.62	131.25	196.87				459.37	525.0	590.62	656.25	721.87		853.12	
Experiment (two disks with loader)	OUTER	BPFO	98.43			393.75			787.5	885.93	984.37	1082.8			1279.6	
		BPFI	164.06			656.25		984.37	1148.4		1476.5	1640.6	1804.6			
		BSF	65.62	131.25				393.75			656.25	721.87	787.5			
	INNER	BPFO	98.43	196.87					689.06		984.37	1082.8	1181.2	1279.6		
		BPFI	164.06					984.37	1148.4			1804.6		2132.8		
		BSF	65.62	131.25	196.87											
	BALL	BPFO	196.87					590.62		787.5	885.93		1082.8	1181.2		
		BPFI				656.25	820.31			1312.5				1968.7	2132.8	
		BSF														
	COMB	BPFO	98.43	196.87				590.62	689.06	787.5		984.37		1181.2		
		BPFI	164.06				820.31	984.37	1148.4	1312.5			1804.6		2132.8	
		BSF	65.62	131.25					459.37	525.0	590.62		721.87	787.5	853.1	

Table 6. The harmonics of defected bearing elements frequencies for running speed 33 Hz.

Table 7 shows that the increased shaft running speed will raise the bearing defect frequencies and decrease the bearing life. Also the defect frequencies with increased amplitude of harmonics appear in the vibration spectrum data. In Table 4 and 5, the defects frequencies and their harmonics were not found effectively for lower running speed when no loader attached to the shaft. The harmonics of frequencies for running speed 41 Hz was found to be quite distinct in comparison to running speed 17 , 25, and 33 Hz.

The defects frequencies of the ball bearings in the COMB case for running speed 41 Hz are shown in Fig. 3, 4, 5, 6, 7, and 8. The parallel dotted lines indicate the locations of bearing defect characteristic frequency and its harmonics.

The vibration amplitude is in the gPk scale. When the normal state of the REB was operated properly, the vibration was small and constant, however, when the defected REB was operated, there were changes in vibration spectrum as seen in Figures for the COMB defects case. Figures give amplitude spectrum of the COMB showing the BPFO, the BPFI, and the BSF for shaft running speed 41 Hz with or without loader respectively. Fig. 3 and 4 give defect frequency of 121.8 Hz and its harmonic frequencies such as 243.7, 365.6, and so on for the BPFO. Fig. 5 and 6 give defect frequency of 203.1 Hz and its harmonic frequencies such as 406.2, 609.3, and so on for the BPFI. Fig. 7 and 8 give defect frequency of 81.25Hz and its harmonic frequencies such as 162.5, 243.7, and so on for the BSF.

		Running Speed		Corresponding Frequency (xHz)												
		41 Hz		x1	x2	x3	x4	x5	x6	x7	x8	x9	x10	x11	x12	x13
Calculated	With Defect	BPFO	125.1	250.2	375.4	500.5	625.7	750.8	875.9	1001.1	1126.2	1251.4	1376.5	1501.6	1626.8	
		BPFI	202.8	405.7	608.5	811.4	1014.2	1217.1	1419.9	1622.8	1825.7	2028.5	2231.4	2434.2	2637.1	
		BSF	81.6	163.3	244.9	326.6	408.2	489.9	571.6	653.2	734.9	816.5	898.2	979.9	1061.5	
	GOOD	BPFO	2.08	4.16	6.24	8.33	10.41	12.49	14.57	16.66	18.74	20.82	22.91	24.99	27.07	
		BPFI	3.38	6.76	10.14	13.53	16.91	20.29	23.68	27.06	30.44	33.83	37.21	40.60	43.98	
		BSF	1.36	2.72	4.08	5.44	6.80	8.16	9.52	10.88	12.25	13.61	14.97	16.33	17.69	
	Experiment (two disks without loader)	OUTER	BPFO	121.8	243.7	365.6	487.5			853.1	975	1096.8		1340.6	1462.5	1584.3
			BPFI	203.1	406.2		812.5	1015.6		1421.8	1625				2437.5	2640.6
			BSF	81.2	162.5	243.7	325.0	406.2	487.5	568.7	650.0		812.5		975.0	
INNER		BPFO		243.7		487.5		731.2								
		BPFI				812.5	1015.6		1421.8	1625.0		2031.2	2234.3		2640.6	
		BSF	81.25	162.5	243.7	325.0		487.5		731.2	812.5		975.0	1056.2		
BALL		BPFO	121.8	243.7	365.6		609.3	731.2	853.1			1218.7	1340.6	1462.5	1584.3	
		BPFI	203.1	406.2	609.3			1218.7	1421.8	1625.0	1828.1	2031.2	2234.5	2437.5	2640.6	
		BSF	81.2	162.5	243.7		406.2		568.7	650.0	731.2		893.7			
COMB		BPFO	121.8	243.7	365.6	487.5	609.3	731.2	853.1	975.0	1096.8	1218.7		1462	1584	
		BPFI	203.1	406.2	609.3		1015.6	1218.7	1421.8	1625.0	1828.1	2031.2	2234.3	2437.5		
		BSF	81.2	162.5	243.7	325.0	406.5	487.5	568.7		731.25	812.5	893.7	975.0		
Experiment (two disks with loader)		OUTER	BPFO	121.8	243.7	365.6	487.5	609.3	731.2	853.1	975.0	1096.8	1218.7	1340.6		
			BPFI	203.1	406.2	609.3			1218.7							2640.6
			BSF	81.2	162.5	243.7	325.0	406.2	487.5	568.7	650.0	731.2		893.7	975.0	
		INNER	BPFO	121.8	243.7		487.0	609.3	731.2	853.1	975.0		1218.7	1340.6		
			BPFI	203.1	406.2	609.3			1218.7			1828.1	2031.2			
			BSF	81.2		243.7	325.0	406.2	487.5	568.7	650.0			893.7	975.0	1056.2
	BALL	BPFO	121.8	243.7	365.6	487.5	609.3					1218.7	1340.6	1462.5	1584.3	
		BPFI	203.1	406.2	609.3		1015.6	1218.7		1625.0	1828.1		2237.5	2437.5	2640.6	
		BSF	81.2	162.5	243.7	325.0	406.2	487.5	568.7					1056.2		
	COMB	BPFO	121.8	243.7	365.6	487.5	609.3	731.2		975.0		1218.7		1462.5		
		BPFI	203.1	406.2	609.3			1218.7				2031.2	2234.3		2640.6	
		BSF	81.25	162.5	243.7	325.0	406.2	487.5	568.7	650.0	731.2		975.0			

Table 7. The harmonics of defected bearing elements frequencies for running speed 41 Hz.

Fig. 9 and 10 illustrate the vibration data of inboard bearing housing for the GOOD and the COMB cases and outboard bearing housing for normal state bearing in the vertical and horizontal directions using multiple channels in one graph. The frequency range was 0-5 kHz. The spectrum of the GOOD and the COMB cases with loader in vertical direction (CH 3) represents resonance around 3 kHz. It is probably the accelerometer excitation effect. It is known that some of specified bearing defect frequencies can be damped by surrounding structure more than others and this case may cause frequencies to resonate.

Thus, natural frequencies of bearing housing and bearing elements or accelerometer can excite to cause resonance. It can be noted that the peak values of amplitude of both the GOOD and the

COMB cases with loader were much lower than no loader attached for higher shaft running speed.

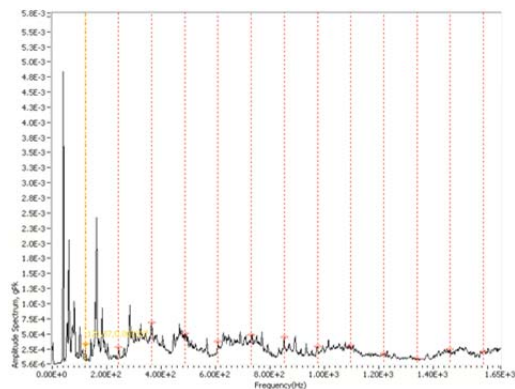


Figure 3. Amplitude spectrum of the COMB for the BPFO at 41Hz without loader.

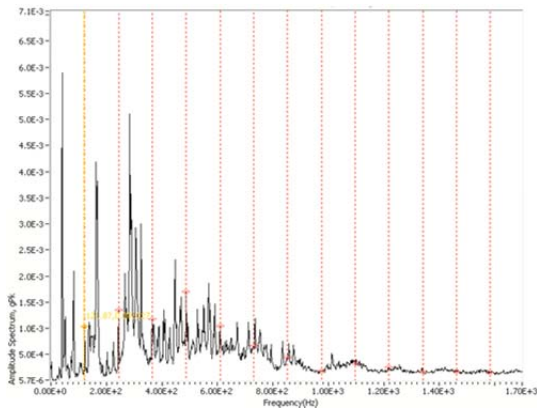


Figure 4. Amplitude spectrum of the COMB for the BPFO at 41Hz with loader.

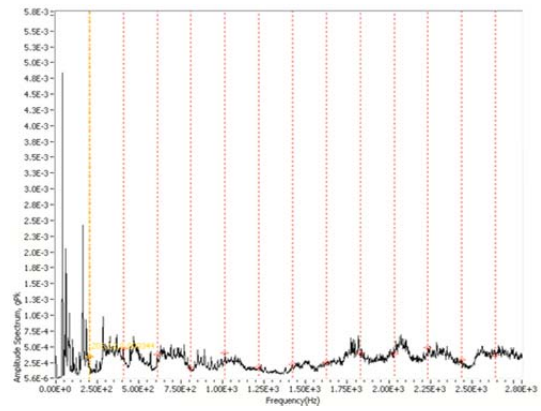


Figure 5. Amplitude spectrum of the COMB for the BPFI at 41Hz without loader.

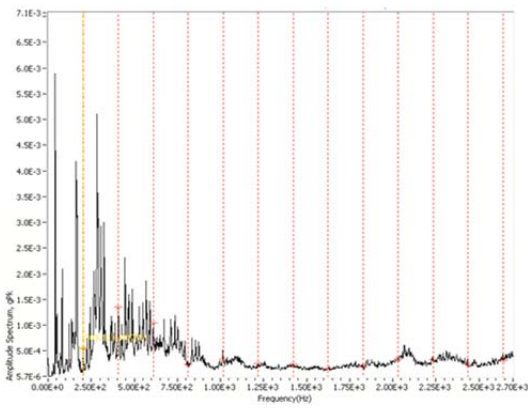


Figure 6. Amplitude spectrum of the COMB for the BPFI at 41Hz with loader.

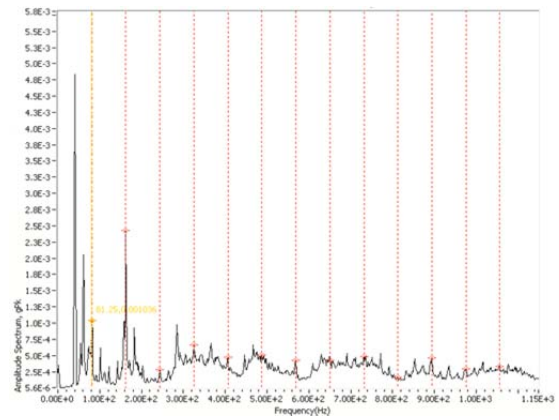


Figure 7. Amplitude spectrum of the COMB for the BSF at 41Hz without loader.

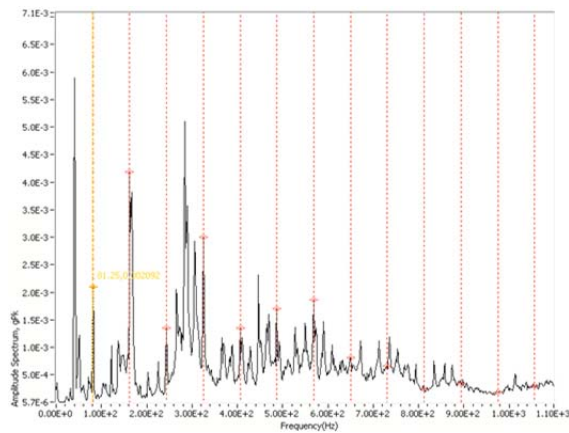


Figure 8. Amplitude spectrum of the COMB for the BSF at 41Hz with loader.

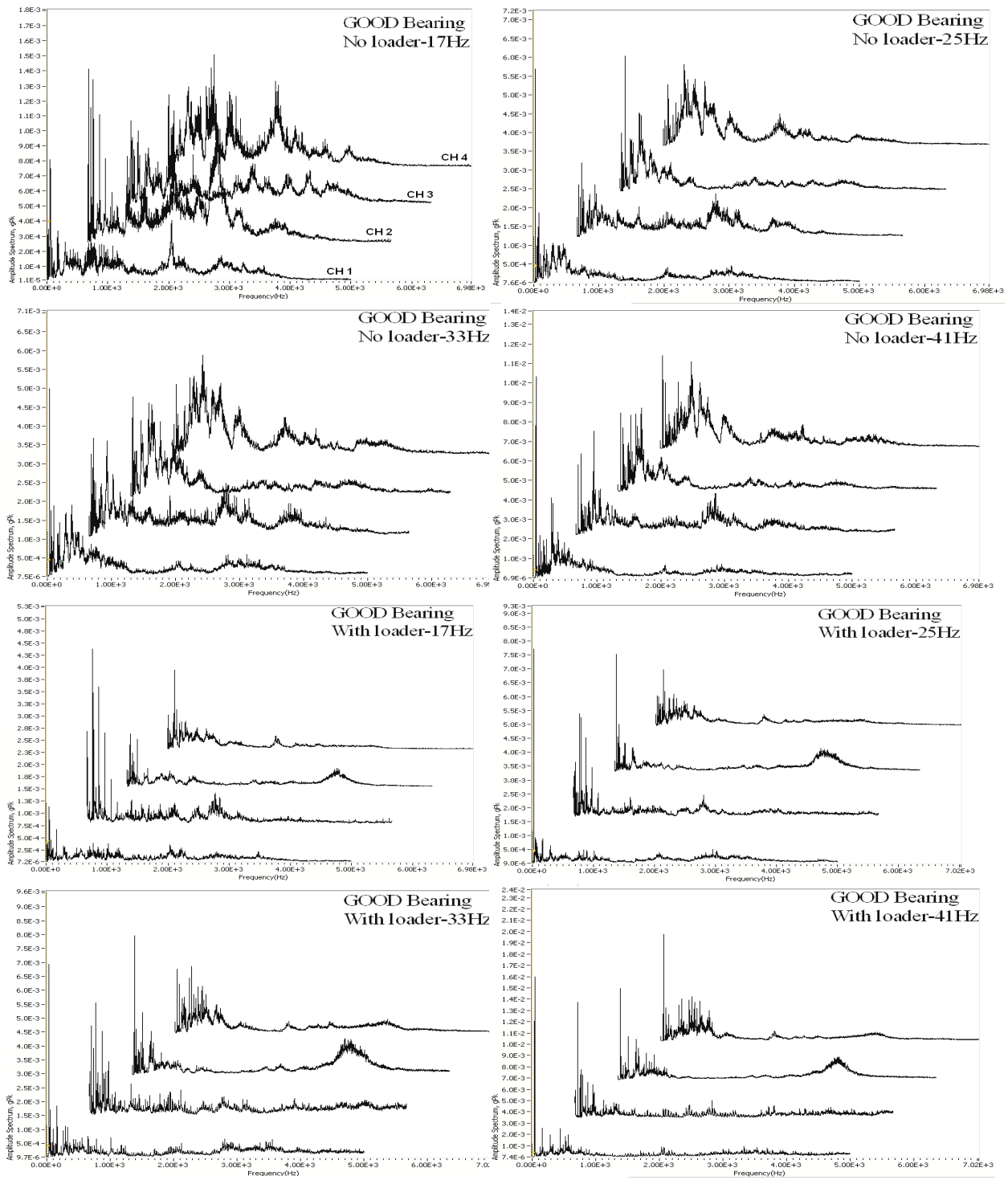


Figure 9. Amplitude spectrum (0.5 ~5 kHz) of the GOOD bearing for running speed 17, 25, 33, and 41 Hz with and without loader.

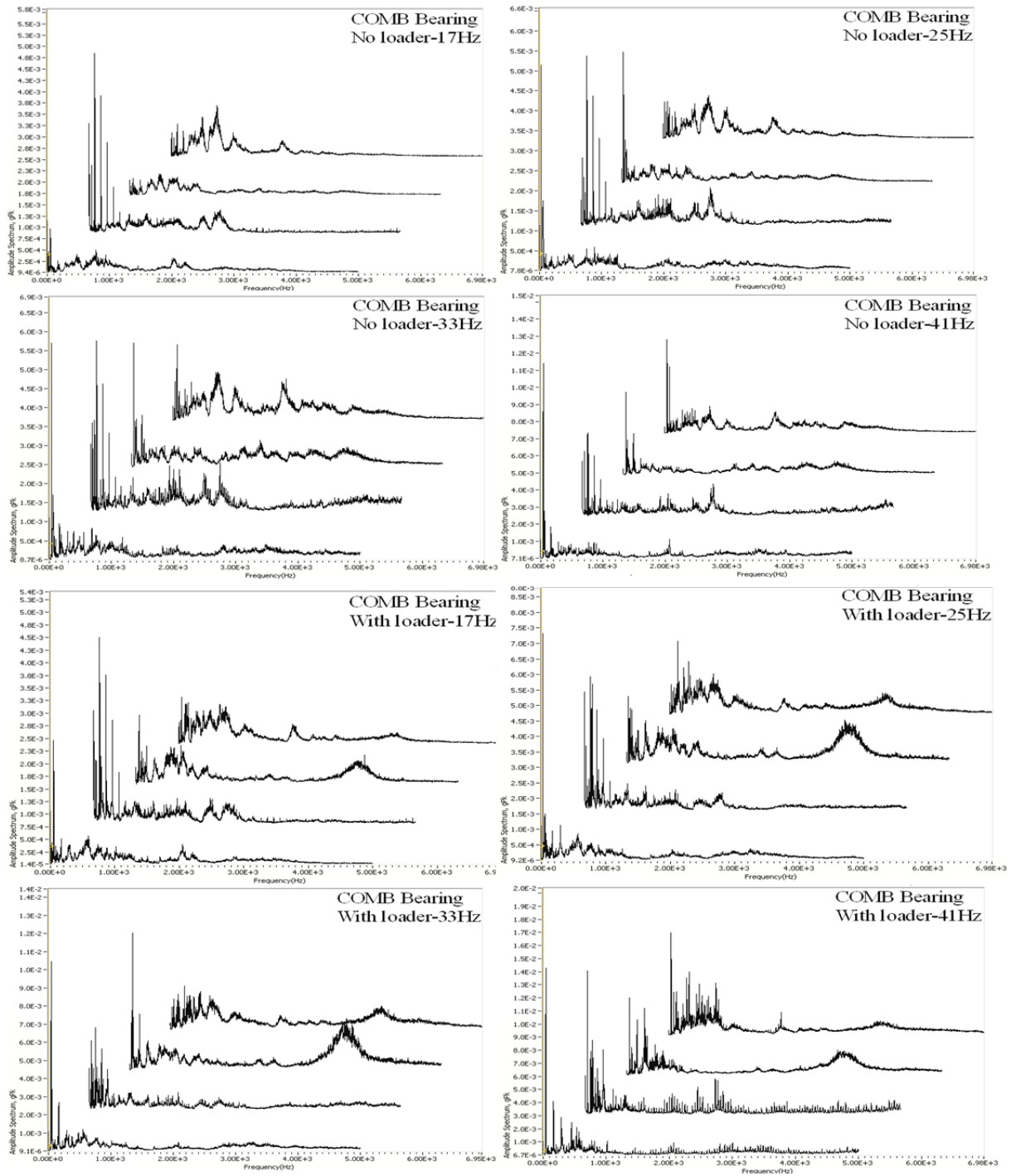


Figure 10. Amplitude spectrum (0.5 ~5 kHz) of the COMB bearing for running speed 17, 25, 33, and 41 Hz with and without loader.

5. Conclusions

One of the most important mechanical components to take into account is the REB due to its vital function on the dynamic behavior of most rotating machinery. Rotating machineries are complex and have numerous components that could potentially fail. A large majority of these components rely on the REB for continued successful operation. One way to increase operational reliability is to monitor defects in the REBs. One of the most effective techniques to use for condition monitoring of the REB is vibration spectrum analysis. Vibration analysis is a critical for condition monitoring to find the location, cause, and severity of defects. In this study, normal state condition bearing and deliberately defected bearings were tested under different shaft running speeds (17 Hz, 25 Hz, 33 Hz, and 41 Hz) with two load levels. The data collected during running tests were observed, analyzed, and presented in detail but to put all findings here is limited due to the length of this paper.

Acknowledgements

The authors would like to acknowledgement the support of the University of Düzce for the project entitled BAP-2010.03.02.042. The authors gratefully thank professor Ismail Ercan for his assistance.

References

- [1] P. Kadarno, Z. Taha, T. Dirgantara, K. Mitsui, Vibration analysis of defect ball bearing using finite element model simulation, 9th Asia Pacific Industrial Engineering & Management System Conference, APIEMS (2008) 2832-2840.
- [2] J. Chebil, M. Hrairi, N. Abushikhah, Signal analysis of vibration measurements for condition monitoring of bearings, Australian Journal of Basic and Applied Sciences, 5(1) (2011) 70-78.
- [3] Z. Kırıl, H. Karagülle, Vibration analysis of rolling element bearings with various defects under the action of an unbalanced force, Mechanical Systems and Signal Processing, 20 (2006) 1967-1991.
- [4] S.A. Abduslam, F. Gu, A. Ball, Bearing fault diagnosis based on vibration signals, Proceedings of Computing and Engineering Annual Researchers Conference (2009) 93-98.
- [5] T. Doğuer, J. Strackeljan, P. Tkachuk, Using a dynamic roller bearing model under varying fault parameters, 6th International Conference on Condition Monitoring and Machinery Failure Prevention Technologies (2009) 907-918.
- [6] M. Elforjani, D. Mba, Condition monitoring of slow-speed shafts and bearings with acoustic emission, Strain, Int.J.for Experimental Mechanics (2010) 1-14.
- [7] A. Muthukumarasamy, S. Ganeriwala, The effect of frequency resolution in bearing fault studies, Technote, SpectraQuest Inc. 2010.
- [8] H. Wang, P. Chen, Fault diagnosis method based on kurtosis wave and information divergence for rolling element bearings, WSEAS Transactions on System 8(10) (2009) 1155-1165.
- [9] M. Kunli, W. Yunxin, Fault diagnosis of rolling element bearing based on vibration frequency analysis, 3rd International Conference on Machinery Technology and Mechatronics Automation, IEEE, Computer Society (2011) 198-201.
- [10] J.I. Taylor, Identification of bearing defects by spectral analysis, Mechanical Design 102 (1980) 199-204.
- [11] T. Igarashi, H. Hamada, Studies on the vibration and sound of defective rolling bearings, Bulletin of the Japan Society of Mechanical Engineers, 25 (1989) 248-253.